Stockholms universitet

Modelling and Simulation the Growth of Neuronal Dendrites in 3-Dimensional Space

Fatemeh Zamanzad Ghavidel

Masteruppsats i matematisk statistik
Master Thesis in Mathematical Statistics

Masteruppsats 2010:5
Matematisk statistik
December 2010

www.math.su.se

Matematisk statistik
Matematiska institutionen
Stockholms universitet
106 91 Stockholm

Stockholm University

Mathematical Statistics
Stockholm University
Master Thesis **2010:5**
http://www.math.su.se

Modelling and Simulation of the Growth of Neuronal Dendrites in 3-Dimensional Space

Fatemeh Zamanzad Ghavidel*

December 2010

Abstract

The Morphological development of neurons is a very complex process involving both cellular and molecular mechanisms. Computational modelling and numerical simulation of neuronal morphology are invaluable tools for understanding evolvement procedures and structurefunction relationships. The aim of this project is to apply and develop methods of stochastic modelling, Markov chains, for simulating the dendritic morphology of brain neurons in 3-dimensional domains. We examine how dendritic elongation, branching and termination tips in pyramidal neurons are controlled by the birth and death process, with the number of growing dendrites as its state and the appropriate growth, birth, bifurcatioand termination rates. Pyramidal neurons consist of three different kinds of dendrites in terms of their arborisation; namely: 1) basal dendrites, 2) apical and oblique dendrites and 3) tuft dendrites. We present the approach based on the continuous time birth and death process for the basal and tuft dendrites, whereas this method is replaced by a discrete time model for the simulation of apical and oblique dendrites. Simulations are performed to validate each models performance by comparing with the real neuronal cells. It is shown that the models are able to simulate the dendritic arborisation of different parts of pyramidal neuron with respect to the methods described above. These three models are joined after considering the location measurements and a single picture of a pyramidal neuron is created.
Key words: Pyramidal Neurons, Dendritic Arborisation, Markov Chains, Discrete and Continuous Time Birth and Death Process.

*Postal address: Mathematical Statistics, Stockholm University, SE-106 91, Sweden. E-mail:F.Zamanzad@hotmail.com . Supervisor: Mikael Andersson.

Foreword and Acknowledgments

This report constitutes a Master thesis in Biostatistics at the Department of Mathematics at Stockholm University. The project has been proposed by Patrik Krieger at the Department of Neuroscience, Karolinska Institute.

I would like to thank my supervisors Patrik Krieger at Karolinska Institute for presenting this project and his amicable assistance to give me background about the neuroscience field and indeed Mikael Andersson at Stockholm University, who has supported my work with great enthusiastic, valuable suggestions and many hours of worthwhile discussions. Also thanks to all my friends and other people who helped me during this project.

Finally, I owe my loving thanks to my family for their lifelong and heartening support and infinite inspiration.

Fatemeh Zamanzad Ghavidel

Contents

1 Introduction

In the present work we use statistical methods to simulate the 3–dimensional morphology of neuronal dendrites. The morphology of dendrites can be described as a Markov chain, a stochastic process having the Markovian property.

'Different types of neurons can be distinguished by the structure of their dendrites, which can be characterized in terms of segment lengths and diameters, the number of terminals (unbranched tips), the number of branch points, and the topological factors such as symmetry'[1].

Dendritic arborisation underlies many aspects of nervous system structure and is a fundamental substrate of brain activity and functional specialization. Dendrites, along with axons, play a large role in information processing at the single cell level. Many neuroscience studies emphasize the importance of dendritic branching pattern in neuronal behaviour. 'Despite its importance, dendritic branching remains poorly understood. Dendritic branching is driven by a complex interaction of intercellular and extracellular signalling cascades which are proving difficult to completely unravel by molecular biology alone' [2]. Stochastic modelling and computational investigation offer a complementary and enhanced approach to traditional molecular means of uncovering essential properties of dendritic branching. The parameters controlling branching behaviour are measured from real cells, reduced to statistical distributions and methods, which are beneficial to adequately simulate the 3-dimensional structure of neuronal dendrites.

To simulate the morphology of dendrites we have used the method of birth and death process both in continuous and discrete time. Much of our focus has been done to develop separate models for different parts of dendrites in 3–dimensional space.

The samples in this case are taken from the layer 5 of barrel cortex ETV/GLT and visual cortex ETV/GLT in pyramidal neurons of a mouse brain.

Our goal here is the following:

- Develop a model that can be used to simulate dendritic arborisation using the statistical methods mentioned above,
- Estimate the required model parameters directly from measurements

of real dendrites,

- Refine the parameter derivations or basic models assumptions, based on the degree of congruence between real and simulated dendrites.

The entire computational process has been implemented in MATLAB.

The following section illustrates the general structure and definitions of the neurons; in particular pyramidal cells. Section 3 gives the theoretical background of the methods used to simulate the dendritic morphology. Section 4 explains the data which are taken from two kinds of pyramidal neurons. The simulation methods for each separate part of the neuron are clarified in Section 5. Results, simulated models and a single simulated pyramidal neuron are presented in Section 6, and finally in the discussion section we summarize the model and discuss problems and possibilities of further improvements.

2 Background

2.1 Structure of a Typical Neuron

The neuron, also know as a nerve cell, is the core component and the fundamental unit of the nervous system. The basic purpose of a neuron is to receive incoming information and, based upon that information; send chemical and electrical signals to other neurons, muscles, or glands. Neurons are designed to send signals at a very fast rate across physiologically long distances. They do these using nerve impulses or action potentials. Action potentials are electrical charges that change in a wave-like pattern through the length of the nerve cell. When a nerve impulse reaches the end of a neuron, it triggers the release of a chemical; a neurotransmitter. The neurotransmitter travels rapidly across the synapse and acts to signal the adjacent cell.

Although neurons are very diverse and have many different shapes and sizes, most of the nerve cells have some common basic features. Figure 1 illustrates the basic structure of a neuron. A typical neuron in a vertebrate (such as a human) is divided into four major regions: a cell body, dendrites, an axon, and synaptic terminals. Like all cells, the entire neuron is surrounded by a cell membrane. The cell body (soma) is the enlarged portion of a neuron that most closely resembles other cells. It contains the nucleus and other specialized organelles such as the mitochondria, Golgi apparatus, endoplasmic reticulum, secretory granules, ribosomes and polysomes. It provides energy

and coordinates the metabolic activity of the neuron. The dendrites, which branch off in treelike fashion from the cell body, are specialized to receive signals and transmit them toward the cell body. A single neuron may have hundreds of dendrites. An axon is a long, slender projection of a nerve cell that carries signals away from the cell body. Synaptic terminal are at the end of the axon in which neurotransmitter molecules are stored and released. [3]

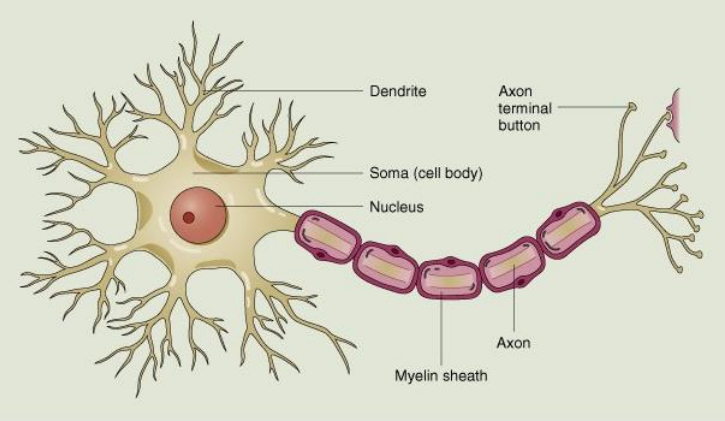

Figure 1: Structure of a typical neuron.[1]

2.2 Pyramidal Neurons

Pyramidal neurons (pyramidal cells) are a type of neuron found in forebrain structures such as the cerebral cortex, hippocampus, and amygdala, but not in the olfactory bulbs, striatum, midbrain, hindbrain, or spinal cord. They are the most numerous excitatory cell types in mammalian cortical structures, suggesting that they play important roles in advanced cognitive functions.

The main structural features of the pyramidal neuron are the triangular shaped soma, or cell body, a single axon, a large apical dendrite, multiple basal dendrites, and the presence of dendritic spines. The basal dendrites emerge from the base and the apical dendrites from the apex of the pyramidal cell body. Dendritic spines receive most of the excitatory impulses that enter a pyramidal cell.

[1]The figure is taken from www.thomasjwestmusic.com/neurologyapplied.htm/.

2.3 Basal and Apical Dendrites

'The structure of pyramidal neurons, although stereotypical, is quite variable, both between regions (e.g. hippocampus vs. neocortex) and within regions (e.g. layer II vs. layer V of neocortex). Nevertheless, pyramidal neurons have a stereotypical morphology, which is best characterized by the presence of separate basal and apical dendritic trees. Several basal dendrites emerge from the base of the pyramidal soma. Each basal dendrite branches up to several times before terminating. The basal dendritic tree appears very similar in form to a stellate neuron (Elston and Rosa, 1998). A single apical dendrite emerges from the apex of the pyramidal soma. In most cases the primary apical dendrite extends for several hundred microns before branching to form an apical tuft, consisting of dendrites that branch a few times before terminating. In some cases the primary apical dendrite bifurcates to form two main apical dendrites. Emanating from the primary apical dendrites are several oblique branches, which typically branch once or twice before terminating. In some cases the primary apical dendrite bifurcates closer to the soma, giving rise to twin apical dendrites, each giving rise to several oblique branches.'

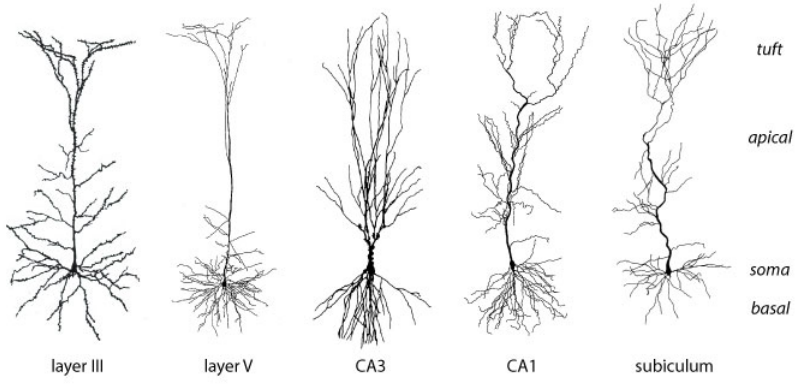

Figure 2: A variety of pyramidal neurons from different parts of the brain.[2]

[2]The article and figure are taken from Scholarpedia. Keyword: 'Pyramidal Neurons'.

3 Methods

3.1 Discrete-time Markov Chain

Consider a stochastic process $\{X_n,\ n = 0, 1, 2, 3, \ldots\}$ that can take a finite or countable number of nonnegative integers. If $X_n = i$, then the process is said to be in state i at time n. Whenever the process is in state i at time n, there is a fixed probability $P_{i,j}$ that the process will be in state j at time $n + 1$. We suppose that

$$P\{X_{n+1} = j | X_n = i,\ X_{n-1} = i_{n-1}, \ldots, X_1 = i_1, X_0 = i_0\} = P_{i,j}$$

for all states $i_0, i_1, \ldots, i_{n-1}, i, j$ and $n \geq 0$. Such a stochastic process is called a Markov chain. The above equation elucidates that, the conditional distribution of any future state X_{n+1} given the past states $X_0, X_1, \ldots, X_{n-1}$ and the present state X_n is independent of the past states and depends only on the present state.

The value $P_{i,j}$ represents the probability that when the process is in state i, next will make a transition into state j. Probabilities are nonnegative and since the process must make a transition to some state, we have that

$$P_{i,j} \geq 0, \quad i, j \geq 0$$
$$\sum_{j=0}^{\infty} P_{i,j} = 1, \quad i = 0, 1, 2 \ldots$$

Let $\mathbf{P}$ denote the matrix of one-step transition probabilities $P_{i,j}$, so that

$$\mathbf{P} = \begin{Vmatrix} P_{00} & P_{01} & P_{02} & \cdots \\ P_{10} & P_{11} & P_{12} & \cdots \\ \vdots & & & \\ P_{i0} & P_{i1} & P_{i2} & \cdots \\ \vdots & \vdots & \vdots & \end{Vmatrix}$$

3.2 Continuous–time Markov Chain

Consider a continuous time stochastic process $\{X(t), t \geq 0\}$ taking on values in the set of nonnegative integers. We say that the process $\{X(t), t \geq 0\}$ is a continuous–time Markov chain if for all $s, t \geq 0$ and nonnegative integers $i, j, x(u),\ 0 \leq u < s$

$$\begin{aligned} p\{X(t+s) = j | X(s) = i, X(u) = x(u),\ 0 \leq u < s\} \\ = P\{X(t+s) = j | X(s) = i\}. \end{aligned}$$

In other words, a continuous–time Markov chain is a stochastic process having the Markovian property that the conditional distribution of the future $X(t+s)$ given the present $X(s)$ and the past $X(u),\ 0 \leq u < s$, depends only on the present and not on the past.

Moreover, if we let T_i denote the amount of time that the process stays in state i before making a transition into a different state, then

$$P\{T_i > s+t | T_i > s\} = P\{T_i > t\}$$

for all $s, t \geq 0$. The random variable T_i is memoryless and is exponentially distributed.

According to the above equation we can define a continuous-time Markov chain in another way namely; a stochastic process which has the properties that each time it enters state i

(i) The amount of time it spends in that state before making a transition into a different state is exponentially distributed with mean $1/\nu_i$.

(ii) When the process leaves state i, it next enters state j with a probability $P_{i,j}$ satisfying

$$P_{i,i} = 0 \quad \text{all } i$$
$$\sum_j P_{i,j} = 1 \quad \text{all } i.$$

In addition, the amount of time the process spends in each state, must be conditionally independent given the sequence of entered states.

3.3 Birth and Death Process

Consider a system whose state at any time is represented by the number of people in the system at that time. Whenever there are n people in the system, then (i) new arrivals enter the system at an exponential rate λ_n and (ii) people leave the system at an exponential rate μ_n. That is, whenever there are n persons in the system, then the time until the next arrival is exponentially distributed with mean $1/\lambda_n$ and is independent of the time until the next departure which is itself exponentially distributed with mean $1/\mu_n$. This system is called a birth and death process, which has wide applicability in the study of biological system. The parameters $\{\lambda_n\}_{n=0}^{\infty}$ and $\{\mu_n\}_{n=1}^{\infty}$

are called respectively the arrival (or birth) and departure (or death) rates.

The birth and death process is a continuous–time Markov chain with states $0, 1, 2, \ldots$ for which transitions from state n may go either to state $n-1$ or state $n+1$. The relationship between the birth and death rates, the state transitions rates and probabilities are:

$$\begin{aligned} v_0 &= \lambda_0, \\ v_i &= \lambda_i + \mu_i, \quad i > 0 \\ P_{01} &= 1, \\ P_{i,i+1} &= \frac{\lambda_i}{\lambda_i + \mu_i}, \quad i > 0 \\ P_{i,i-1} &= \frac{\mu_i}{\lambda_i + \mu_i}, \quad i > 0 \end{aligned}$$

When there are i individuals in the system, then the next state will be $i+1$ if a birth occurs before a death; and the probability that an exponential random variable with rate λ_i is smaller than an (independent) exponential with rate μ_i is $\lambda_i/(\lambda_i + \mu_i)$ and the time until the first event occurs is exponentially distributed with rate $\lambda_i + \mu_i$. The preceding results follow from the properties of the exponential distribution which is discussed more in the Appendix.

The birth and death process can also be described as a discrete–time Markov chain, where at each discrete time point a birth and / or death may occur. Suppose $X_n = i$, then, $X_{n+1} = i + 1$ or, $X_{n+1} = i - 1$. That is, state transitions are always between neighbouring states.

4 Data

The samples in this project are taken from the barrel cortex ETV/GLT and visual cortex ETV/ GLT of layer 5 pyramidal cells. Morphometric specification of these two cortical cell types in L5 pyramidal neuron will be discussed more in the Appendix.

In principle, the neuron can be represented by points in three-dimensional space connected to each other through edges. For instance, if there is an edge between two points 2 and 3, it means these points are connected to each other by a dendrite. Figure 3 shows how points/edges can be regarded

as a graph representation of the neuron.

Concerning this fact, the data in this case are more in the form of coordinates, and edges connecting corresponding nodes in three-dimensional space. Moreover, there are environmental variables giving the distance between the cell body and other important positions of the pyramidal neuron. The subsequent variables explain more about data.

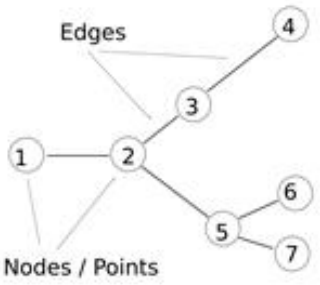

Figure 3: A simple graph with 7 nodes and 6 edges.[3]

Coordinates: The list of three–dimensional coordinates that represent the individual points of the neuron.

Edges: The list of edges which connect points (in no particular order).

Apical root: Index of starting point of apical dendrite tree.

Basal roots: The list of starting points of basal dendrites.

Branch points: The list of all points that branch off from the parent dendrites.

Terminal points: The list of all points where dendrites terminate (stop growing).

Soma coordinates: Three–dimensional coordinates where the cell body or soma is located; this is normalized so that the soma is always set to be at $(0, 0, 0)$. This is the location where all dendritic trees start growing.

[3]The figure is taken from Wikipedia. Keyword: 'Graph'.

Soma L4L5: The distance from cell body to layer4-layer5 border, the location where layer 4 ends and layer 5 begins. Dendritic growth is different in layer4 and layer5. Specifically, layer4 has almost no dendrites, apart from the long apical dendrite that grows straight upwards and the number of the oblique dendrites in this layer is thus limited.

Soma pia: The distance from soma to pia (top of the brain). This is a physical upper bound for neuronal growth; the neuron cannot grow above this level.

Soma wm: The distance from soma to white matter (bottom of the brain area). This is a lower bound for neuronal growth, but neurons do not usually grow much in this direction.

Intermediate segment lengths: Basal intermediate segment lengths for all barrel cortex ETV/GLT and visual cortex ETV/GLT.

Terminal segment lengths: Basal terminal segment lengths for all barrel cortex ETV/GLT and visual Cortex ETV/GLT.

Histograms in figure 4 and 5 show descriptive features of ETV–pyramids in terms of basal intermediate and terminal segment lengths.

In addition, particular parts of the pyramidal neuron, which are mentioned in section 2.3, grow in different layers. Basal dendrites together with the cell body emerge in layer 5, while oblique dendrites appear in layer 4 and tuft dendrites emanate from the upper 10% of the pia–white matter distance in barrel cortex and upper 15% of the pia–white matter distance in visual cortex pyramidal neurons [4]. This corresponds almost to the layer1-layer2 border. The data about approximate layer depth from pia and thickness is available in the Appendix.

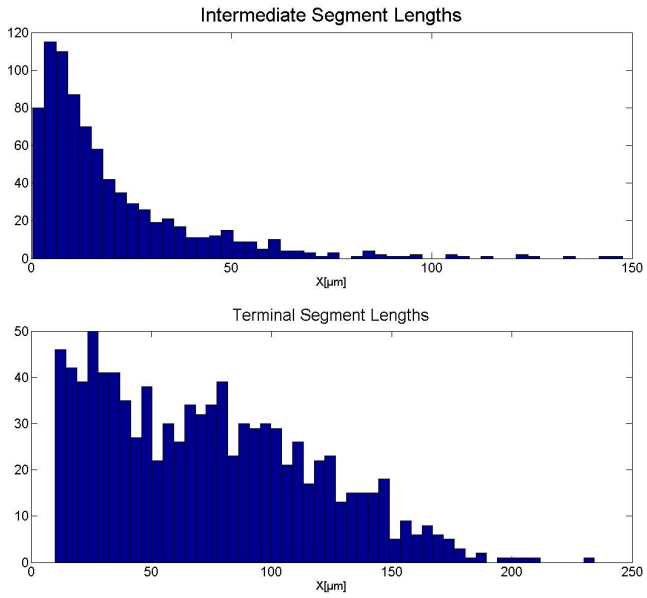

Figure 4: Basal segments lengths in barrel cortex ETV.

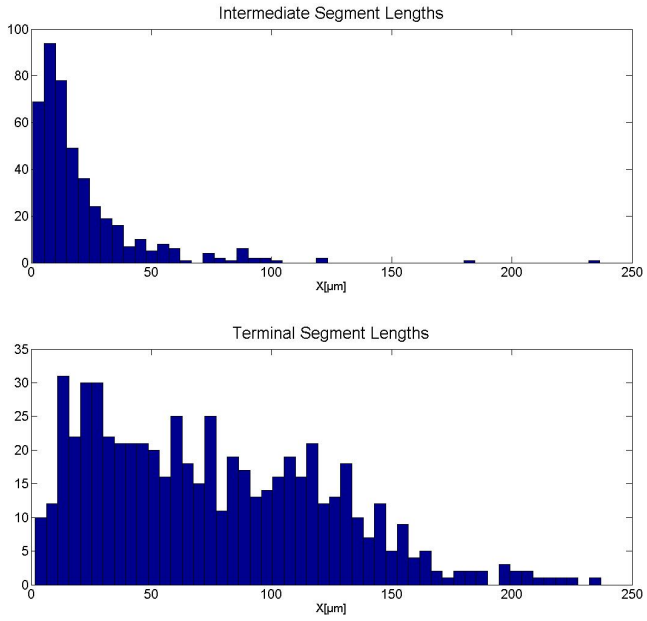

Figure 5: Basal segments lengths in visual cortex ETV.

5 Model for the Pyramidal Cell

5.1 Model Background

Due to the morphological characteristics of layer 5 pyramidal neurons, in terms of different dendritic arborisation and distinctive layers among them, whole dendrites in pyramidal cells can be divided into three separate regions:

- Cell body and basal dendrites in layer 5,
- Obliques dendrites along with apical in layer 4,
- Tuft dendrites which branch off from the top of the apical. They start approximately from layer1–layer2 border and elongate near to pia.

Assume that dendritic growth in each section mentioned above proceeds independently of each other during the whole process. This fact leads us to implement separate procedures with respect to each region.

One common method of simulation, which is used here, is to apply birth and death processes for each part independently. The procedure used for basal and tuft dendrites is based on the continuous-time birth and death process, while we change the method to discrete time for the apical and oblique dendrites in layer 4 as an approximation of the continuous case . During the growth process of dendrites the following events can occur at each section independently:

- Birth event: When a new basal dendrite emerges from the cell body, a new oblique dendrite grows from the apical, or a new tuft dendrite emanates from the apical.
- Bifurcation event: When a parent dendrite branches into two other (daughter) dendrites.
- Termination event: When a dendrite (new birth or branch) stops growing.

Moreover, the probability of occurrence of each event is denoted by P_{birth}, P_{branch}, and $P_{\text{termimate}}$.

According to the above events growth rates, birth rates, bifurcation rates and termination rates are considered as the parameters of the birth and death processes. For simplicity, same symbols are used for all birth rates, bifurcation rates and termination rates in different regions. Table 1 illustrates the possible rates with their symbols used during model building.

Table 1: Rates and symbols.

	Basal	Apical/Oblique	Tuft
Growth rate	λ_b	λ_o	λ_t
Birth rate	τ	τ	τ
Bifurcation rate	γ	γ	γ
Termination rate	ν	ν	ν

The basal and tuft growth rates are regarded as constant values and set equal to one during the whole period of the simulation. This is mainly due to the lack of data for different times of the neuronal growth process that creates difficulties for estimating the growth rates. Since the main objective of the simulation process is to create a realistic image of the final neuron, the simulation time is adjusted to achieve this. By letting $\lambda_b = \lambda_t = 1$ we do not include them in our models anymore.

The number of growing dendrites (G) at any time is considered as the state of the Markov process for each section. Possible values of this state is denoted by the set of nonnegative integers $\{0, 1, 2, 3 \ldots\}$. Transitions from state n may go either to state $n-1$ or state $n+1$, except for $n = 0$ from which it is only possible to go to $n = 1$. This transition is based on the probabilities of occurrence for each possible event.

5.2 Model Descriptions

5.2.1 Basal and Tuft Dendrites

The method applied for the basal and tuft dendrites is based on a continuous–time birth and death process and are almost identical to each other, so the same procedure is mentioned for both parts. The flow chart in figure 6 shows the model for getting the number of growing dendrites $G(i)$ which is related to the event probabilities at each step.

The stochastic growth process starts with 0 dendrites and the next event will be a new birth. After observing the first event as a new birth, the second event can be a bifurcation or termination of the first dendrite or independently another dendrite is born and grows. The fate of the dendrite to end in either a branch or a termination or to continue as a new birth is determined stochastically using the corresponding transition probabilities.

For this purpose, a uniformly distributed random variable $(0 < R < 1)$ is generated and compared with $P_{\text{terminate}}$. The first newborn dendrite will be ended in a termination if $R < \nu/(\tau+\gamma+\nu)$, and the number of the growing dendrites will change to 0. If this condition is not satisfied the next event will be branching or bifurcation. Another value of R is generated and compared with P_{branch}. If $R < \gamma/(\tau+\gamma)$ the event will be a bifurcation, otherwise another newborn will be added to our system. In both cases the number of the growing dendrites will increase by one. This algorithm will continue by considering the number of growing dendrites at the time when one of the possible events occurs. Denote the number of growing dendrites at the beginning of the model by $G(0) = 0$. The number of growing dendrites after the ith event where $i \geq 1$, is defined as $G(i)$. The probabilities of the next occurring events directly depend on the number of growing dendrites at each step, so the probability of termination for the $i+1$th event will be

$$\frac{G(i)\cdot\nu}{(\tau+G(i)\cdot(\gamma+\nu))}$$

and the probability of bifurcation given that termination has not occurred, is

$$\frac{G(i)\cdot\gamma}{(\tau+G(i)\cdot\gamma)}.$$

At each termination event the number of growing dendrites is decremented by 1, while if the process leads to either a bifurcation or a new birth, G is incremented by 1. Denote the time of the first event (new birth) by T_1. Further, for $i > 1$ let T_i denote the elapsed time between the events $i-1$ and i. T_i for $i = 1, 2, 3, 4, \ldots$ are conditionally independent given the sequence of visited states and have exponential distribution with mean

$$\frac{1}{(\tau+G(i-1)\cdot(\gamma+\nu))}.$$

Let $S_i = T_1 + T_2 + \cdots + T_i$, which is the waiting time until the ith event happens. For simplicity consider S_i as the start time of the ith event and denote it by T_{start}.

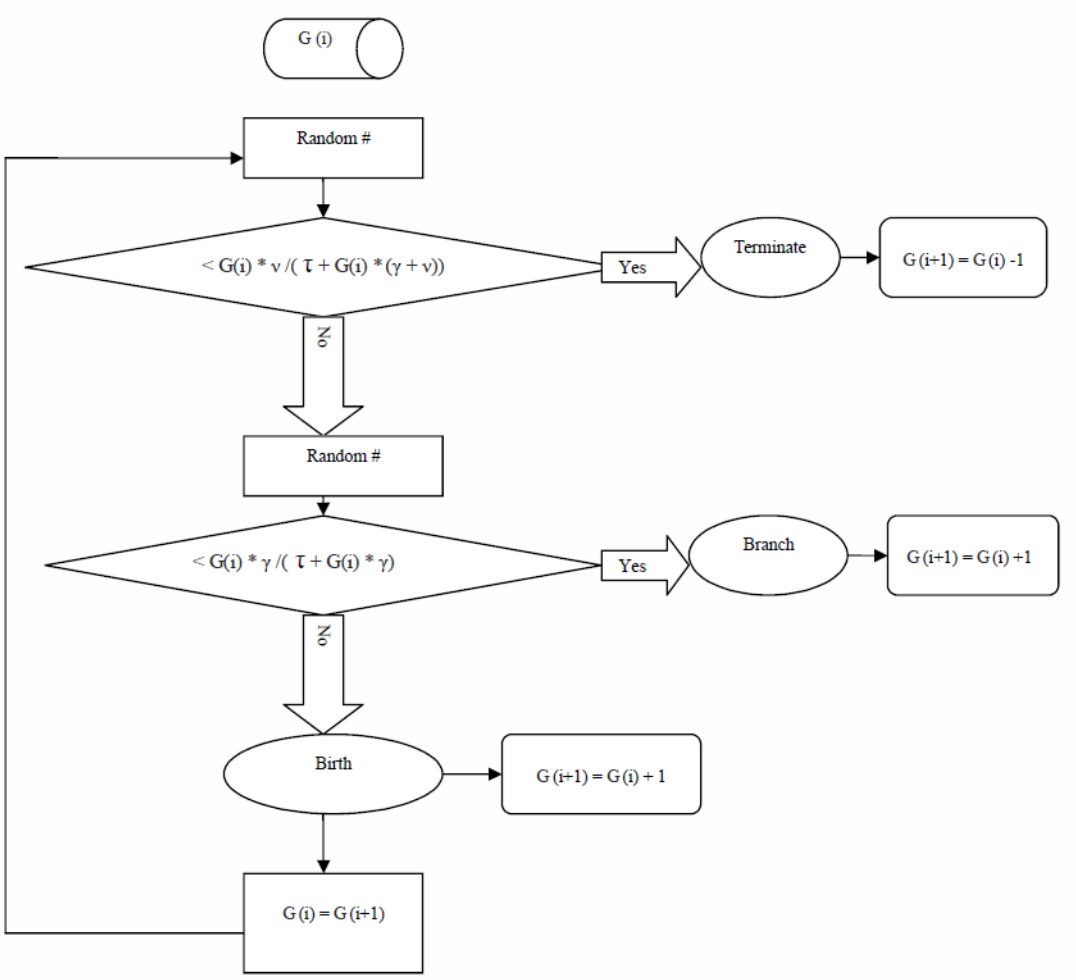

Figure 6: Flow chart of the basal and tuft dendrites growth process.
Input at the initiation of the process is the number of growing dendrites $G(i)$. Random # refers to a random number drawn from a uniform distribution between 0 and 1.

5.2.2 Apical and Oblique Dendrites

By looking at the morphology of the apical dendrite in a real neuronal cell, which grows from the apex of the soma and elongates straight upwards, we imagine the apical as the Z-axis that emanates from the origin $(0, 0, 0)$, the position of the soma. The newborn oblique dendrites can start growing at

any position on the apical. The number of oblique dendrites becomes greater as the length of the apical increases, in other words, when the length of the apical becomes larger, the probability of an oblique dendrite being born will increase. This fact leads us to conclude that instead of having constant rate we should consider a linear growth rate $\lambda_o t$, where t is the current time of the process. Note that $\lambda_o t$ is the length of the apical from the cell body at time t. Using the linear rate, the time until the next event does not follow the exponential distribution (see the Appendix). In order to overcome this problem, we have used a discrete-time Markov chain and applied the model to the whole layer 4 of pyramidal cell. By dividing the period of time into very tiny and small intervals of length dt we can consider the discrete–time birth and death process as an approximation of the underlying continuous process. The number of growing oblique dendrites G is the state of the process at each tiny interval.

By considering t as the current time of our process, which increases stepwise with the quantity dt, the probabilities of a new birth, a bifurcation and a termination per unit dt calculated using the following formulas:

$$\begin{aligned} P_{\text{birth}} &= \tau \cdot \lambda_o \cdot t \cdot dt \\ P_{\text{branch}} &= \gamma \cdot G(t) \cdot dt \\ P_{\text{terminate}} &= \nu \cdot G(t) \cdot dt \end{aligned}$$

The process starts at time $t = 0$ when there are no oblique dendrites in the model, $G(0) = 0$. The next event will be the newborn oblique dendrite which will occur at a specific discrete time point according to the birth probability.

The flow chart in figure 7 shows the algorithm for getting the number of growing oblique dendrites per dt unit. The time interval dt is assumed to be so small that all transition probabilities are small as well.

In order to get the occurrence time of each specific event from the beginning of the process we just need to input a start value of $T_{\text{start}} = t \cdot dt$ which indicates the start time of the events.

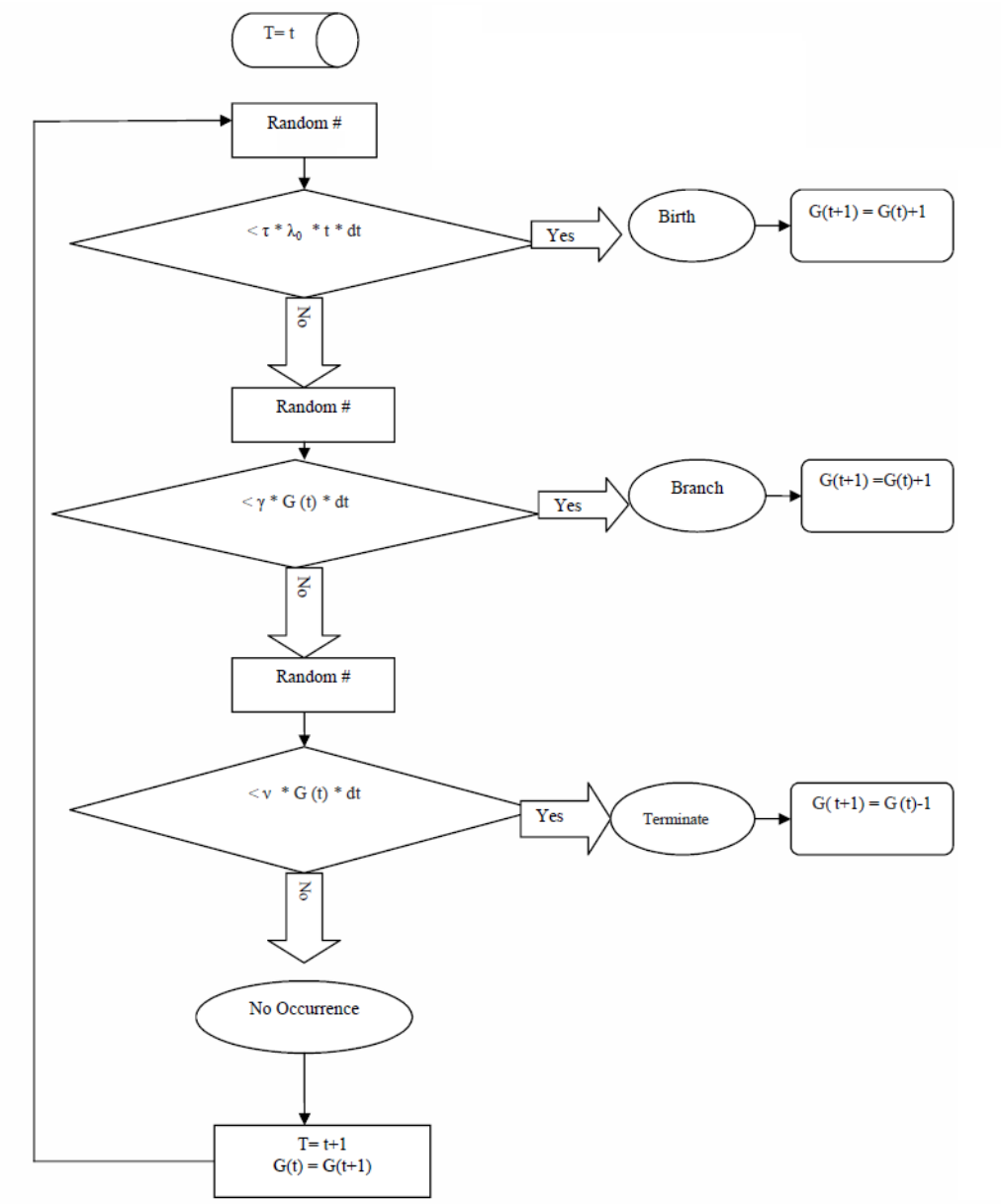

Figure 7: Flow chart of the oblique dendrites growth process.
Input at the initiation phase is the start time of the process. Random # refers to a random number drawn from a uniform distribution between 0 and 1.

5.3 Stopping Times

After obtaining the time point when a particular event starts, the next step is to find the stopping time of the new birth or bifurcation event. For example, if we have one newborn dendrite with starting time, say, T_{start}, the next step is to get the time this dendrite branches into two other dendrites or stops growing. This time is defined as the stopping time or simply T_{stop}. Note that the starting time of one branching dendrite is equal to the stopping time of its parent dendrite, which can be a new birth or a bifurcation itself. Also the termination event can be related to one new birth or branching dendrite as well. Broadly speaking, in order to get the stopping time for the new birth and branching dendrites, at each bifurcation or termination event with $T_{\text{start}} = L$, one new birth or bifurcation with $T_{\text{start}} = S$, where $S < L$, is selected randomly. The starting time L will be the T_{stop} of the dendrite with $T_{\text{start}} = S$. This procedure will continue until all new birth and branching dendrites have their own stopping times.

5.4 Coordinates

Figure 8 shows the real picture of a barrel (somatosensory) cortex from a mouse brain projected in two–dimensional space. The scale is in micrometers for both the X and Y axes. Each dendrite can be determined by its starting and stopping coordinates. Also the starting coordinates of each branch are the same as the stopping coordinates of its parent dendrite.

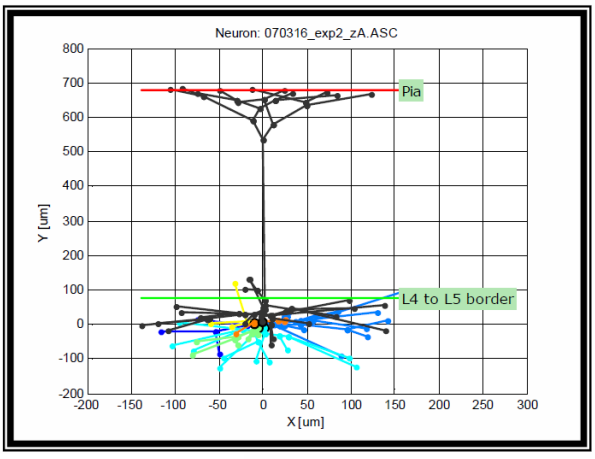

Figure 8: Real neuronal picture in two–dimensional space.

In order to get the starting and stopping coordinates for each newborn or branching dendrite, three other variables such as position coordinates, direction coordinates and angles have been defined in such a way that along with T_{start} and T_{stop} assist us to get the specific coordinates of each dendrite. In the following we describe how these variables are calculated for each individual dendrite.

- Position coordinates are the starting coordinates of each dendrite and this variable have specific values for the newborn dendrite in each section separately.

  (i) By denoting the coordinates of the cell body as $(0, 0, 0)$, the starting coordinates for the newborn basal dendrites will be $(0, 0, 0)$.

  (ii) Regarding the apical as a Z–axis, as mentioned in Section 5.2.2, each new oblique from apical (new birth) will be at one point along the Z–axis, so the position coordinates of each newborn oblique dendrite is $(0, 0, z)$ where $z = \lambda_o \cdot t \cdot dt$.

  (iii) The position coordinates of the newborn tuft dendrites are equal to the coordinates where the apical stops growing.

- The direction coordinates which are calculated from the spherical coordinates system are :

$$\begin{aligned} X &= \rho \sin\Phi \cos\theta \\ Y &= \rho \sin\Phi \sin\theta \\ Z &= \rho \cos\Phi. \end{aligned}$$

- The angular variables are defined in spherical coordinates, ρ is the radius and is set to one; Φ is the polar angle from the positive Z–axis with $0^\circ \leq \Phi \leq 180^\circ$ (π rad) and θ is the azimuthal angle in the XY–plane from the X–axis with $0^\circ \leq \theta < 360^\circ$ (2π rad). However, the azimuth θ is often restricted to the interval $(-180^\circ, 180^\circ]$. The spherical coordinates system is discussed thoroughly in the Appendix.

The angles have special statistical distributions for each newborn and bifurcation dendrites. Φ_{birth} has a normal distribution with parameters depending on the dendritic shapes and their angles from the positive Z–axis, and θ_{birth} is uniformly distributed on the open interval $(-180^\circ, 180^\circ)$, because of cylindrical symmetry. The proper parameters of the distribution of Φ_{birth}

are discussed separately for each region in Section 6.

Bifurcation dendrites do not have a large variation from their parents in terms of angles and direction. According to this fact, Φ_{branch} and θ_{branch} have normal distributions with parameters which are dependent on the parent dendrite. Possible parametrization are discussed in more detail in Section 6.

Therefore, as mentioned above we have the following general distributions for each section with the specific parameters that depend on the dendritic growth shapes which differ widely at each region.

$$\Phi_{\text{birth}} \sim \text{Normal distribution}(\mu, \sigma)$$
$$\theta_{\text{birth}} \sim \text{Uniform distribution}(-180^\circ, 180^\circ)$$

$$\Phi_{\text{branch}} \sim \text{Noraml distribution}(\Phi_{\text{parent}}, \sigma)$$
$$\theta_{\text{branch}} \sim \text{Noraml distribution}(\theta_{\text{parent}}, \sigma)$$

After getting the relevant values of direction variables for each dendrite, the stopping coordinates can be calculated from the following formulas for basal and tuft dendrites:

$$\text{stopping coordinates} = \text{position coordinates} + \text{direction coordinates} \cdot \Delta T$$

where ΔT is $T_{\text{stop}} - T_{\text{start}}$. For oblique dendrites the corresponding formula is:

$$\text{stopping coordinates} = \text{position coordinates} + \text{direction coordinates} \cdot \lambda_o \cdot \Delta T.$$

5.5 Edges

In order to distinguish which dendrites are connected to each other during the growth process, T_{start} and T_{stop} of different dendrites are taken into account. In other words, if the T_{start} of one arbitrary dendrite is the same as T_{stop} of another dendrite, then we can conclude that there is an edge between them which connects these two dendrites. T_{start} and T_{stop} of all dendrites examined and the possible edges assembled at the end of comparison are stored in a matrix with the number of rows equal to the number of edges and two columns. Then, the dendrite in each row is connected to another in such a way that the edge extends from the dendrite which is placed in the

first column, thereby helping us to get the direction of the edges between dendrites. If one dendrite has two edges that extend from it, then this point represents a parent dendrite which branches into two other daughter dendrites. Note that the stopping coordinates of the parent dendrite is the same as the starting coordinates of its two branches.

After getting all edges of the process, the next step is to connect the coordinates of dendrites according to the edge matrix. We perform this process for the separate parts of the neuronal cell. So, at the end, there will be three sets of edges with their corresponding coordinates.

5.6 Combining Three Models

After getting the separate edges and coordinates for basal, oblique and tuft dendrites, we can combine edges and coordinates together and make a single picture of the pyramidal cell. By considering the approximate value of layers, the apical dendrite elongates from the cell body in layer5a–layer5b border and stops growing close to the layer1–layer2 border. This length is the difference between layer5a–layer5b border and layer1–layer2 border. When the apical dendrite ends, tuft dendrites start growing and the starting coordinates of the new birth tuft dendrites are $(0, 0, 574)$. Notice that the scale is in μm.

6 Model Simulations

6.1 Basal Dendrites Simulations

The shapes of the basal dendrites from the real neuronal cells guide us to determine suitable values of the parameters for the distribution of angles. The newborn basal dendrites grow downwards from the cell body. According to these facts, we have selected Φ_{birth}, the polar angle of basal growth directions, to have a normal distribution. The majority of the newborn basal dendrites grow along the negative part of the Z–axis and we have a few number of dendrites with large deviations from this direction. Thus the mean value of the normal distribution is decided to be 180° with a standard deviation of 45°, which indicates the deviation of dendrites from the negative part of the Z–axis.

Φ_{branch} and θ_{branch} have normal distributions with the parents' angles as their mean values. By examining some different values as a standard deviation of the branching angles distributions, the suitable parameter is chosen to be 10 degrees which has the most contingency with the real neuronal shapes. So, the appropriate models for the basal dendrites in layer 5 are:

$$\Phi_{\text{birth}} \sim \text{Normal distribution}(180^\circ, 45^\circ)$$
$$\theta_{\text{birth}} \sim \text{Uniform distribution}(-180^\circ, 180^\circ)$$

$$\Phi_{\text{branch}} \sim \text{Noraml distribution}(\Phi_{\text{parent}}, 10^\circ)$$
$$\theta_{\text{branch}} \sim \text{Noraml distribution}(\theta_{\text{parent}}, 10^\circ)$$

By increasing the standard deviation σ of the Φ_{branch} and θ_{branch} distributions, the bifurcation dendrites deviate more from their parents dendrites. Figure 9 depicts this fact clearly. This algorithm was run until time $t = 100$. The values of the new birth, bifurcation and termination rates are selected in such a way that the simulated model shows the suitable consistency with the real pyramidal neuron, thus we choose $\tau = 3, \gamma = 4$ and $\nu = 4$. By changing the rates of the model we will have different pictures of the simulation. For instance, by increasing the bifurcation rate, the results display basal parts with more branches.

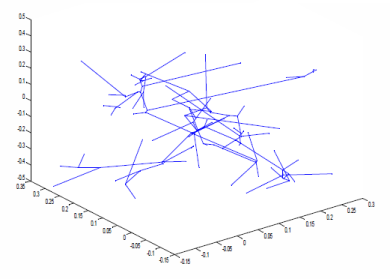

(a) Basal dendrites with $\sigma = 80°$.

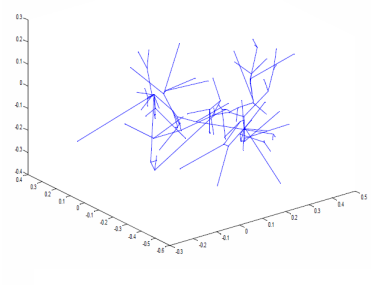

(b) Basal dendrites with $\sigma = 60°$.

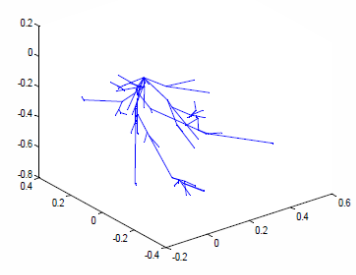

(c) Basal dendrites with $\sigma = 30°$.

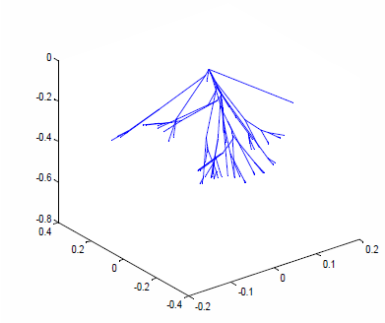

(d) Basal dendrites with $\sigma = 10°$.

Figure 9: Simulated basal dendrites with different σ.

The number of growing basal dendrites of the simulated figure 9(d) is shown as a stairstep graph in figure 10. The first newborn dendrite starts to grow when $T_{\text{start}} = 0.219$ and the process continues until the number of growing basal dendrites reaches 36 when $T_{\text{start}} = 0.758$. This simulated model results in 6 newborn basal dendrites, 62 bifurcations and 32 terminal points.

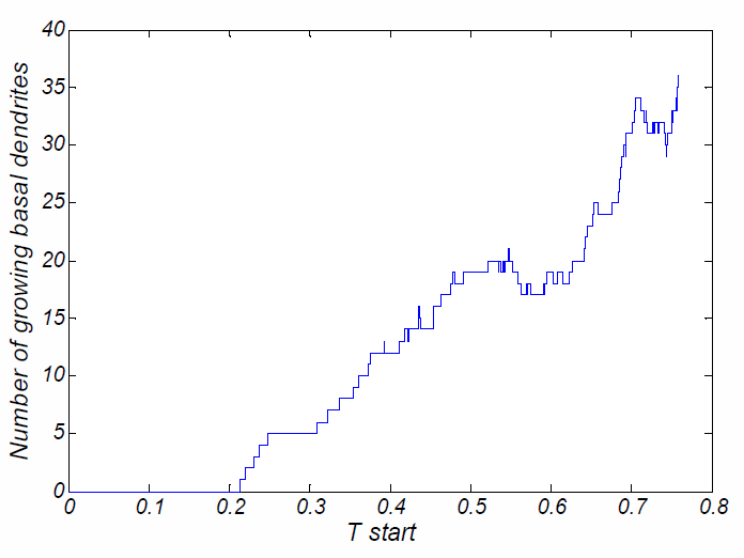

Figure 10: Stairstep graph of the growing basal dendrites.

6.2 Apical and Oblique Dendrites Simulations

As mentioned before, we consider the apical dendrite to grow in the direction of the Z–axis in three–dimensional space. Newborn oblique dendrites grow from all sides of the apical, the majority of them have approximately 90 degrees angles from the Z–axis. We have decided to consider a normal distribution with mean 90 degrees and standard deviation 3 degrees for the newborn oblique dendrites. The angle distributions for branches have normal distributions whose mean parameters are dependent on the parents' dendrite. Thus the following represent the suitable distributions in layer 4:

$$\Phi_{\text{birth}} \sim \text{Normal distribution}(90^\circ, 3^\circ)$$
$$\theta_{\text{birth}} \sim \text{Uniform distribution}(-180^\circ, 180^\circ)$$

$$\Phi_{\text{branch}} \sim \text{Noraml distribution}(\Phi_{\text{parent}}, 3^\circ)$$
$$\theta_{\text{branch}} \sim \text{Noraml distribution}(\theta_{\text{parent}}, 3^\circ)$$

Choosing a small rate for the τ as a parameter helps us to obtain the suitable picture. The growth rate of the apical is set to be $2/5$ in order to get the best realistic figure of apical length. Figure 11 shows how dendritic morphology changes with different rates and assists to choose the best graphs. The apical

dendrite grows from the cell body $(0, 0, 0)$ and elongates till $(0, 0, 574)$. Time for this algorithm run until 50 and dt is set to be 0.01.

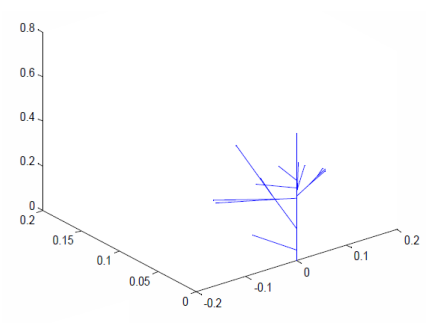

(a) $\tau = 1, \gamma = 3$ and $\nu = 3$.

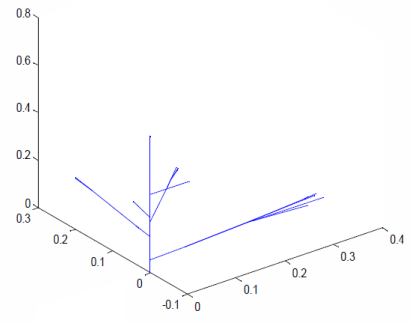

(b) $\tau = 0.8, \gamma = 6$ and $\nu = 5$.

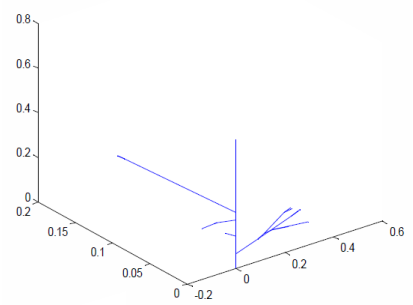

(c) $\tau = 0.1, \gamma = 6$ and $\nu = 5$.

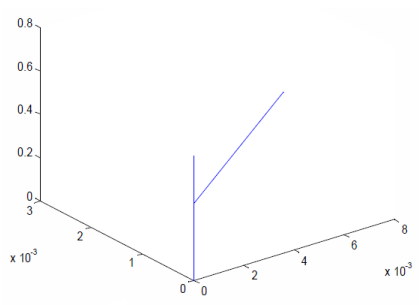

(d) $\tau = 0.01, \gamma = 4$ and $\nu = 5$.

Figure 11: Simulated apical and oblique dendrites with different rates.

6.3 Tuft Dendrites Simulations

Tuft dendrites start to branch out from the top part of the apical which approximately corresponds to the layer1–layer2 border. The newborn dendrites grow up along the Z–axis. Normal distribution with the mean value 80 degrees and standard deviation 5 degrees are selected for the Φ_{birth} distribution, since the majority of the newborn dendrites grow nearly 80 degrees from the Z–axis. The angles for bifurcations have normal distributions with a standard deviation of 5 degrees, which shows the highest consistency with

the real tuft dendrites. Appropriate distributions for tuft dendrites are:

$$\Phi_{\text{birth}} \sim \text{Normal distribution}(80^\circ, 5^\circ)$$
$$\theta_{\text{birth}} \sim \text{Uniform distribution}(-180^\circ, 180^\circ)$$

$$\Phi_{\text{branch}} \sim \text{Noraml distribution}(\Phi_{\text{parent}}, 5^\circ)$$
$$\theta_{\text{branch}} \sim \text{Noraml distribution}(\theta_{\text{parent}}, 5^\circ)$$

The pictures below show the simulated tuft dendrites with different rates. The time horizon for this simulation is $t \in [0, 100]$.

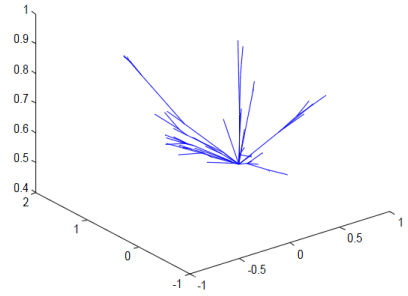

(a) $\tau = 1, \gamma = 3$ and $\nu = 3$.

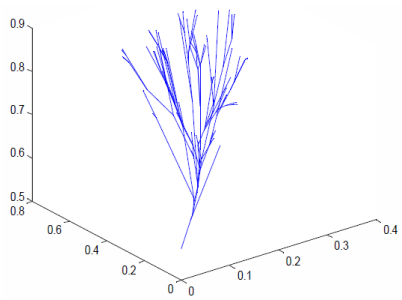

(b) $\tau = 3, \gamma = 5$ and $\nu = 3$.

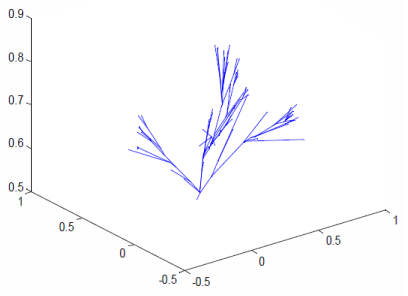

(c) $\tau = 6, \gamma = 4$ and $\nu = 3$.

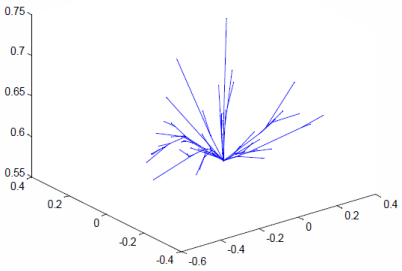

(d) $\tau = 6, \gamma = 5$ and $\nu = 5$.

Figure 12: Simulated tuft dendrites with different rates.

The graph below shows the stairstep plot of the simulated figure 12(d). The model results in 11 newborn dendrites, 43 bifurcations and 46 terminal points.

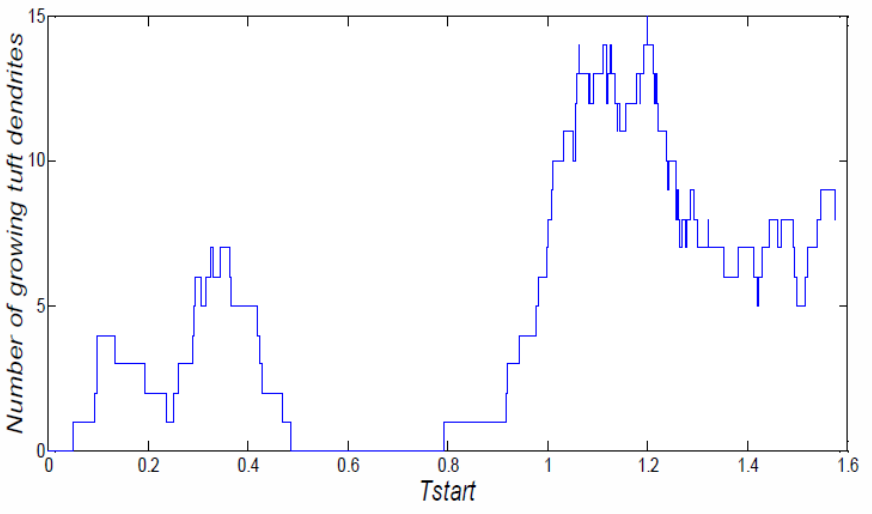

Figure 13: Stairstep graph of the growing tuft dendrites.

6.4 Single Picture of Neuron

Combining the three models will result in a complete picture of a pyramidal cell. This combination has been done according to the layer depth discussed in earlier sections. The figures below show the single picture of neurons in three–dimensional space.

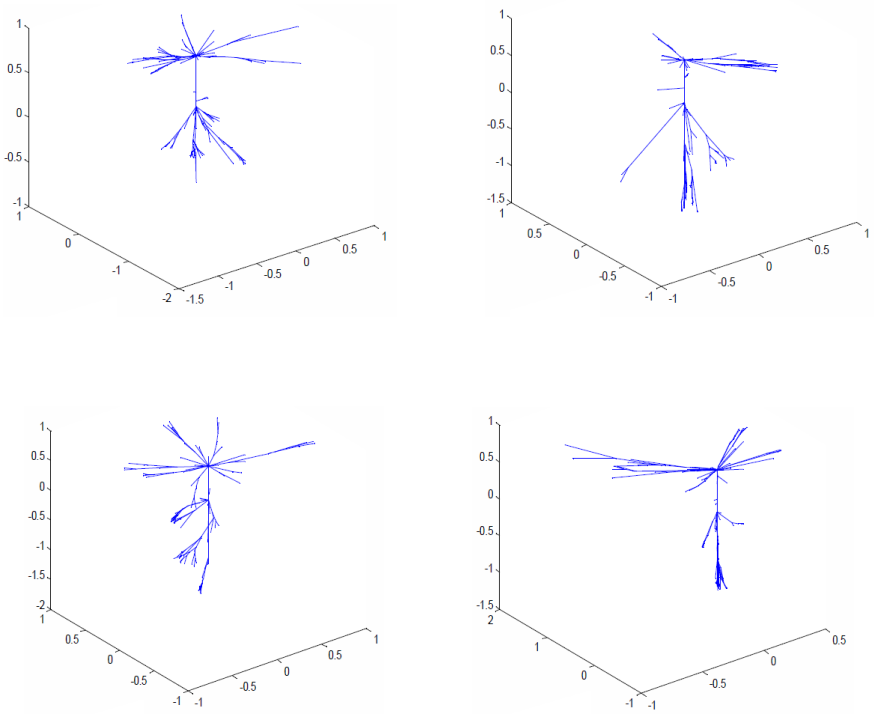

Figure 14: Simulated pyramidal neurons.

7 Discussion

7.1 Aim

The aim of this project has principally been to perform a computational investigation based on the stochastic modelling of birth and death process and simulate the dendritic morphology of a pyramidal neuron in three-dimensional domains, where the model parameters are all extracted from experimental data. On the basis of our simulation in MATLAB, three separate models work well and show satisfactory results in the sense of fulfilling our expectations and the degree of congruence between real and simulated

dendrites.

Dendritic development is a complex process. Stochastic modelling and numerical simulation are powerful tools to help us understand this complicated procedure. Many previous models of dendritic arborisation vary widely in both their methodology in terms of the specific algorithm such as Hidden Markov Models [5] or Monte Carlo simulations [6], and the choice of the morphometric variables like the number of bifurcations, branch order, branch start diameters, radius, the path distance from the soma and intermediate or terminal segment lengths.

7.2 Data

The experimental data are taken from two kinds of L5 pyramidal neuron at specific time point, when the neuronal growth is almost completed. The problem occurs when the neuronal morphometric structures are based on one data set at a particular time point. The growth rates of dendrites in different parts of the cell are not constant and in order to estimate the growth rates we need morphometric measurements at different time points during the whole growth process of the neuron. Due to this lack of data the growth rate of the basal and tuft dendrites assumed to be constant and equal to 1.

Especially the importance of this issue attracts attention where the linear growth rate $\lambda_o t$ has a better fit to the layer 4 of pyramidal cell but in this case the conditions of the continuous-time Markov chain are not satisfied. A reasonable approach in this situation is to apply a discrete–time Markov chains and assume the growth rate to be constant.

7.3 Further Studies

By describing the morphometric measurements of GLT and ETV pyramidal neurons such as the number of nodes in basal dendrites, tuft width, the number of oblique dendrites and the apical length, the possibility of the next studies will be neuronal simulation in terms of specific kinds of cells. Also the relevant rates can be estimated from the experimental data directly. For example, by considering the time scale of the process until the dendritic

growth is completed, the point estimates of the parameters are as follows:

$$\text{Birth rate} = \frac{\text{Number of new births dendrites}}{\text{Whole time of the process}}$$

$$\text{Bifurcation rate} = \frac{\text{Number of bifurcation dendrites}}{\text{Whole time of the process}}$$

$$\text{Termination rate} = \frac{\text{Number of termination tips}}{\text{Whole time of the process}}.$$

8 References

[1] Graham, B.P and Van Ooyen, A.(2006) Mathematical modelling and numerical simulation of the morphological development of neurons, *BMC Neuroscience, Vol. 7,* 1-12.

[2] Donohue, D.E and Ascoli, G.A. (2008) A Comparative Computer Simulation of Dendritic Morphology. *PLoS Computational Biology, Vol. 4,* 1-15.

[3] www.biologyreference.com/Mo-Nu/Neuron.html.

[4] Groh, A. et al. (2010) Cell-Type Specific Properties of Pyramidal Neurons in Neocortex Underlying a Layout that Is Modifiable Depending on the cortical area. *Celebral Cortex, Vol. 20,* 826-836.

[5] Samsonovich, A. V and Ascoli, G.A.(2005) Statistical Determinants of Dendritic Morphology in Hippocampal Pyramidal Neurons:A Hidden Markov Model. *Hippocampus, Vol. 15,* 166-183.

[6] Burke, R. E. et al.(1992) A Parsimonious Description of Motoneuron Dendritic Morphology Using Computer Simulation. *Journal of Neuroscience, Vol. 12,* 2403-2416.

9 Appendix

9.1 Further Properties of the Exponential Distribution

(i) Suppose that X_1 and X_2 are independent exponential random variables with means $1/\lambda_1$ and $1/\lambda_2$ respectively. Then the probability that X_1 is smaller than X_2 is $\lambda_1/(\lambda_1+\lambda_2)$.

This probability is calculated by conditioning on X_1

$$\begin{aligned} P\{X_1 < X_2\} &= \int_0^\infty P\{X_1 < X_2 | X_1 = x\}\lambda_1 e^{-\lambda_1 x}\, dx \\ &= \int_0^\infty P\{x < X_2\}\lambda_1 e^{-\lambda_1 x}\, dx \\ &= \int_0^\infty e^{-\lambda_2 x}\lambda_1 e^{-\lambda_1 x}\, dx \\ &= \int_0^\infty \lambda_1 e^{-(\lambda_1+\lambda_2)x}\, dx \\ &= \frac{\lambda_1}{\lambda_1+\lambda_2}. \end{aligned}$$

(ii) Suppose that $X_1, X_2, X_3, \ldots, X_n$ are independent exponential random variables, with X_i having rate $\mu_i, i = 1, 2, \ldots, n$. The smallest of the X_i is exponentially distributed with a rate equal to the sum of the μ_i. This is shown as follows:

$$\begin{aligned} P\{\min(X_1, X_2, X_3, \ldots) > x\} &= P\{X_i > x \text{ for each } i = 1, 2, \ldots, n\} \\ &= \prod_{i=1}^n P\{X_i > x\} \quad \text{(by independence)} \\ &= \prod_{i=1}^n e^{-\mu_i x} \\ &= \exp\Big\{-\big(\sum_{i=1}^n \mu_i\big)x\Big\}. \end{aligned}$$

9.2 The Inverse Transformation Method

A general method for simulating a random variable having a continuous distribution is the inverse transformation method based on a uniform $(0,1)$ random variable. For any continuous distribution function F if we define the random variable X by

$$X = F^{-1}(U)$$

then the random variable X has a distribution function F. ($F^{-1}(u)$ is defined to equal that value of x for which $F(x) = u$.) Hence, we can simulate a random variable X from the continuous distribution F, when F^{-1} is computable, by simulating a random number U and then setting $X = F^{-1}(U)$.

EXAMPLE. (Simulating an exponential random variable): Consider an exponential random variable X with mean 1. If $F(X) = 1 - e^{-x}$, then $F^{-1}(u)$ is that value of x such that

$$1 - e^x = u$$

or

$$x = -\log(1 - u).$$

Thus, if U is a uniform random variable $(0, 1)$, then

$$F^{-1}(U) = -\log(1 - U)$$

is exponentially distributed with mean 1. Since $1 - U$ is also uniformly distributed on $(0, 1)$, it follows that $-\log U$ is exponential distribution with mean 1.

9.2.1 Linear Rate

Consider an exponential distribution random variable with a linear hazard rate λt. The distribution function of this variable is calculated as

$$\begin{aligned} F(t) &= 1 - e^{-\int_0^t \lambda s ds} \\ &= 1 - e^{-\lambda t^2/2}. \end{aligned}$$

According to the inverse transformation method we have

$$\begin{aligned} e^{-\lambda t^2/2} &= 1 - u \\ -\lambda t^2/2 &= \log(1 - u) \\ t &= \sqrt{\frac{-2\log(1-u)}{\lambda}}. \end{aligned}$$

If U is a uniform random variable $(0, 1)$ then

$$F^{-1}(U) = \sqrt{\frac{-2\log(1-U)}{\lambda}}.$$

As mentioned before $(1 - U)$ is also uniformly distributed on interval $(0, 1)$ so, by comparing the result with the example mentioned above, we notice that $F^{-1}(U)$ does not have an exponential distribution.

9.3 Spherical Coordinates System

In geometry, the spherical coordinate system represents points as a tuple of three components. These components are notated as (ρ, Φ, θ) where ρ represents the radial distance of a point from a fixed origin, Φ represents the zenith angle from the positive Z–axis and θ represents the azimuth angle from the positive X–axis with the region of :

$$\rho \geq 0, \quad 0^\circ \leq \Phi \leq 180^\circ(\pi \text{ rad}), \quad 0^\circ \leq \theta \leq 360^\circ.$$

Any spherical coordinate triplet (ρ, Φ, θ) specifies a single point of three–dimensional space. The three spherical coordinates are converted to Cartesian coordinates by:

$$\begin{aligned} x &= \rho \sin\Phi \cos\theta \\ y &= \rho \sin\Phi \sin\theta \\ z &= \rho \cos\Phi. \end{aligned}$$

Conversely, Cartesian coordinates can be converted to spherical coordinates by:

$$\begin{aligned} \rho &= \sqrt{x^2 + y^2 + z^2} \\ \Phi &= \cos^{-1}\left(\frac{z}{x^2 + y^2 + z^2}\right) \\ \theta &= \tan^{-1}\left(\frac{y}{x}\right). \end{aligned}$$

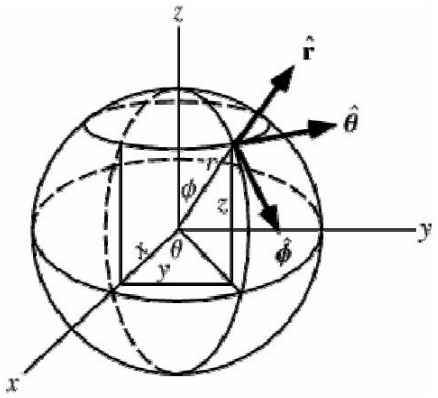

Figure 15: Spherical coordinate system.[4]

[4]Figure 15 is taken from Wolfram MathWorld. Keywords: 'Spherical coordinate systems'.

9.4 Cell–type Specific Properties of Pyramidal Neurons

In rodents, tuft dendrites in layer 5 Pyramidal neurons are classified according to their width. The thick-tufted and the slender–tufted dendrites respond differently to tactile stimuli. The functional difference between these two populations corresponds to two cortical cell types in L5; namely glt– and etv–pyramids. The morphological characteristics of glt and etv–pyramids have been taken into account for each barrel cortex and visual cortex separately.

In barrel cortex, glt–and etv–pyramids corresponds to thick–tufted and slender–tufted pyramidal neuron respectively with the following specifications: Etv–pyramids, compared to the glt–pyramids have a narrower apical tuft dendrite width and fewer primary apical oblique dendrites. The apical dendrite diameter at the base for glt–pyramids is wider than for etv-pyramids. Moreover, for glt–pyramids, the average total apical dendrite length is longer than the average total basal dendrite length. In contrast, for etv–pyramids, the average total apical dendrite length is shorter than the average total basal dendrite length. Compared with glt–pyramids, etv–pyramids have shorter total apical tuft dendrite length, fewer nodes and a smaller width among the most distinguishing morphological parameters. For the basal dendrite, etv–pyramids have more nodes compared to glt–pyramids.

In visual cortex, similar to the barrel cortex for glt–pyramids, the total apical dendrite length is longer than the total basal dendrite length whereas for the etv-pyramids, the total apical dendrite length is shorter than the total basal dendrite length. Etv– and glt–pyramids in visual cortex have on average the same number of obliques as their counterparts in barrel cortex. Etv–pyramids appear as slender–tufted with the shorter total length and narrower width and glt-pyramids as thick tufted pyramidal neurons; Similar to barrel cortex tuft dendrite is the most obvious discriminator between the two call types.[4] Some of the morphological properties of etv– and glt–pyramids in BC and VC are shown in Table 2.

Table 2: Morphological properties of etv– and glt–pyramids in BC and VC.[5]

	BC		VC	
	etv	glt	etv	glt
Tuft width (μm)	157 ± 54	356 ± 84	182 ± 50	290 ± 92
No. of oblique dendrites	3.7 ± 2.2	8.9 ± 2.6	4.1 ± 1.6	9.3 ± 3.9
Total apical tuft length (μm)	944 ± 366	2323 ± 757	1021 ± 421	1784 ± 725
Total basal length (μm)	3006 ± 994	2585 ± 1038	2730 ± 733	2640 ± 792
No. of nodes in basal dendrites	29 ± 11	19 ± 8	22 ± 6	21 ± 7

[5]The table has been adopted from [4], Table 1, page 4.

Figure 16: Pyramidal neurons.[6]

(a) Etv–pyramids in barrel cortex.

(b) Glt–pyramids in barrel cortex.

(c) Etv–pyramids in visual cortex.

(d) Glt–pyramids in visual cortex.

[6]Figure 16 is copied from [4], Supplementary Figure — groh et al.

9.5 Approximate Layer Depth and Thickness in Pyramidal Neurons.

Table 3: Layer thickness and depth from pia = 0.

Layers	Layer thickness (μm)	Layer depth (μm)
L1	93	93
L2	118	211
L3	118	328
L4	233	561
L5a	106	667
L5b	160	827
L6a	200	1026
L6b	84	1111